Real-Time Annealing History of Cold Rolled 3104 Aluminum Alloy

YIH-FARN KAO and SHI-RONG CHEN

New Materials Research & Development Department
China Steel Corporation

An in-situ measuring system correlates the yield stress with an electrical resistivity for the cold rolled 3104 aluminum alloy sheet at various annealing temperatures and soaking times. Based on the fitting level of $R^2 > 0.98$, the resistivity-time curve was proved to be identical with the yield stress-time one at several annealing conditions. The annealing database established via the electrical resistivity indicates a softening history of the sample, and helps mill engineers in optimizing both the annealing time and temperature for the mill product. On the basis of the extended Avrami equations, the activation energy of the recrystallization is found to be 261 kJ/mol which is a reference for the future annealing experiment. This measuring system facilitates the strength targeting for the sample, and therefore is a potential candidate of the commercial instrument to clarify the annealing process.

Keywords: Aluminum alloy, Electrical resistivity, Annealing, Recrystallization, Avrami equation

1. INTRODUCTION

For the production line, the cold-rolled aluminum sheets are manufactured in a number of procedure steps like remelting, casting, hot rolling, cold rolling, and temper annealing. 3104 aluminum alloy is a kind of work-hardening alloy, so the temper annealing process plays an important role on the mechanical properties of final products. For satisfying the customer specification, the mill engineer needs to apply the proper annealing temperature and annealing time under the presupposition of energy saving. Traditionally, the laboratory investigator anneals numerous samples for various times at different temperatures in order to yield an optimized annealing parameter for the mill engineer. However, this way needs a lot of time, human resources, and experience. Therefore an in-situ monitoring is desired to overcome these issues. Differential Scanning Calorimetry (DSC) is widely used to detect the recrystallization temperature of the material, but the obtained temperature is not precise enough and the isothermal annealing is not available. Kazemi-Choob et al. demonstrated that the in-situ electrical resistance measurements could detect the occurrence of the recrystallization process for $Ni_{50.9}Ti_{49.1}$ shape memory wires with different values of cold work[1]. Mukunthan et al. characterized the recovery and the recrystallization processes of the cold-rolled Ti-Nb steel via in-situ X-Ray Diffraction (XRD), and described the isothermal recrystallization kinetics with the Johnson-Mehl-Avrami-Kolmogorov (JMAK) and Speich-Fisher (SF) relationships[2-4]. Unfortunately, the aforementioned methods just specify a rough trend for the annealing process, but in-situ measuring which can reflect the real-time mechanical property is eagerly wanted. This study is aimed at developing a high-resolution in-situ electrical resistivity measurement which can indicate the annealing parameters for producing products that qualify within industrial standards.

2. EXPERIMENTAL METHOD

The 2.2-mm hot-rolled 3104 slab (Al-1.20Mg-1.01 Mn-0.47Fe-0.21Ti-0.20Si-0.17Cu) was fully annealed and consequently cold rolled to 0.29 mm. The 0.29-mm aluminum sheets were cut to the size of 200 × 2.5 × 0.29 mm for in-situ electrical resistivity measurement, 28 × 245 × 0.29 mm for tensile test, 4 × 4 × 0.29 mm for DSC analysis. The instruments for tensile test and DSC are Zwick-Roell 010 and Perkin Elmer-Pyris 1, respectively. The homemade in-situ electrical resistivity measuring system is composed of a four-point AC impedance analyzer and a furnace designed for accurate temperature control. The sample was welded with four isolated tungsten wires, and measured on the holder which was shielded around with the electrical steel, in order to avoid the magnetic disturbance. The optical image of microstructure is obtained via an Olympus-BX53M.

3. RESULTS AND DISCUSSION

3.1 DSC analysis

In order to establish a reference for identical samples before we formally perform the experiment of in-situ resistivity, A DSC measurement is applied to detect the characteristic temperature which is associated with the three stages of the annealing process. Figure 1 shows a compilation of the DSC curves with the heating rates of 20, 10, 5, and 2 ^{o}C/min, respectively. Observed from the data, there are three points worth discussing. First, the characteristic peaks occur at 329 and 318^{o}C when the heating rates = 20 and 10 ^{o}C/min, respectively. The peak temperature shifts to the right with the increased heating rate. For an identical sample, these two peaks are believed to result from the same consequent annealing processes in the lattice, i.e., recovery, recrystallization, and grain growth. When the heating rate was ≤ 5^{o}C/min, one can see that the characteristic peaks disappear in the sinusoidal background. For the mill application, the aluminum coils are always produced with an isothermal soaking. From DSC analysis, the peak shifts with ascending temperature and vanishes at constant temperature make it difficult to find out a proper temperature for isothermal production. Second, the cold-rolled 3104 sheets reveal the recovery behavior when the annealing temperature was ≥ 149^{o}C, while showing the recrystallization and the grain growth behaviors when the annealing temperature was ≥ 204^{o}C in isothermal annealing[5]. However, one can only identify the annealing temperature initially at around 320^{o}C via DSC method, as shown in Fig.1. It implies that the heat transfer of non-isothermal and isothermal conditions are so different that applying the annealing temperature verified from DSC to mill production line was not reliable. Third, the percentage of crystallization is an important issue which manufacturers of aluminum alloy sheets care about. Even for the same type of aluminum alloy, the customers usually request different strength based on various tempers. In addition, manufacturers always try to lower the temperature as much as they can to achieve the required temper for products because of the issue of energy consumption. Besides the temperature, the soaking time is also the key parameter for the annealing process. Unfortunately, the DSC measurement can just inspect if the annealing process happens, but the information of the degree in crystallinity is still lacking. In summary, the precise annealing temperature, the isothermal annealing simulation, and the accurate soaking time for specific temper treatment are the challenges needed to be overcome via in-situ resistivity measurement.

3.2 In-situ electrical resistivity

The sample was arranged with a four-point measurement in the chamber then heated to the target temperature then operated with an isothermal soaking process. The history of the resistivity is shown as Fig.2. Attributed to the nature of positive Temperature Coefficient of Resisti (TCR) in metal material, the resistivity increases with annealing time in 0−290 s. Based on the heating rate of 60^{o}C/min, the Temperature Coefficient of Resistivity (TCR) was estimated to be 0.00193 (^{o}C)$^{-1}$. Illustrated together with related 3xxx and 5xxx series aluminum alloys[6-8], the TCR value equals 0.00510 (^{o}C)$^{-1}$ for Al-1wt%Mg, 0.00193 for Al-1.17 wt%Mg, and 0.00297 for Al-3wt%Mg. Given the phonon vibration suppressed by solute atoms of Mg, the TCR value was reduced when Mg content added increased from 1 to 1.17 wt%. If one further adds Mg to 3wt%, the Al-Mg participations which reveal low resistivity will compromise a part of the suppressed phonon vibration, the existence of TCR ascended from 0.00193 to 0.00297 (^{o}C)$^{-1}$. When the annealing time is > 290 s, the isothermal soaking stage is worth noticing. As shown in Fig.2, the resistivity appears to be in an exponential decay during the isothermal annealing. The decayed resistivity is believed to be resulting from the recovery, the recrystallization, and the grain growth processes in the lattice. Hence the resistivity data acquired from the isothermal soaking period will be elucidated in detail in the following paragraph. The overall decay of percentage in resistivity due to these three stages of the annealing process is usually less than 2.5%, so the electronic signal must be clean enough for later investigation. Fortunately, our measuring system with extremely high resolution in resistivity (~50 nΩ) makes it possible to quantitatively verify these three stages of the annealing process in lattice. It is also worth mentioning that we intentionally increased the heating rate from 60 to 200 ^{o}C/min for the following regular experiments in order to avoid the unexpected recovery behavior under the soaking temperature.

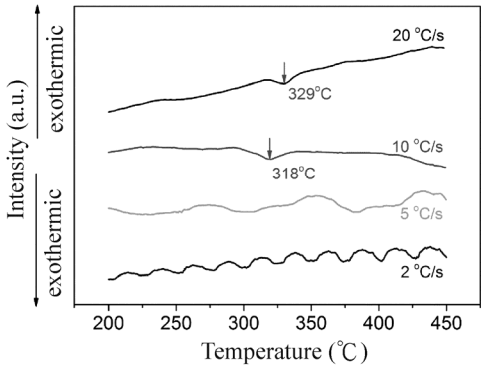

Fig.1. DSC profiles measured with the heating rates of 20^{o}C/min, 10^{o}C/min, 5^{o}C/min, and 2^{o}C/min, respectively.

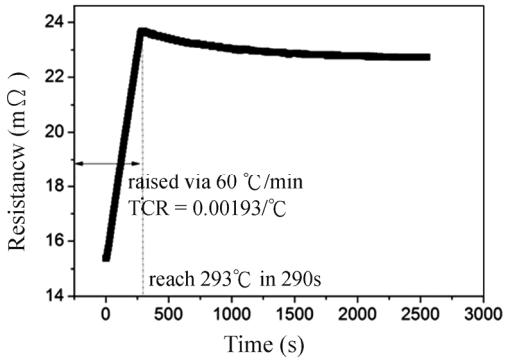

Fig.2. An example of the electrical resistance history annealed at 293°C.

3.3 Resistivity and yield stress

The raw data of resistivity and yield stress obtained from the same aluminum sheet will be normalized by the correlation as follows:

$$\frac{R_{instant} - R_{final}}{R_{initial} - R_{final}} = \frac{Y_{instant} - Y_{final}}{Y_{initial} - Y_{final}} = C \quad \text{..... (1)}$$

where $R_{instant}$ is the resistivity during the isothermal annealing process, $R_{initial}$ is the resistivity at the beginning of the isothermal annealing process, R_{final} is the resistivity at the end of the isothermal annealing process, $Y_{instant}$ is the yield stress during the isothermal annealing process, $Y_{initial}$ is the yield stress of the beginning of the isothermal annealing process, Y_{final} is the yield stress of the end of the isothermal annealing process, and C is coloration index between resistivity and yield stress. Figure 3(a) displays the C vs. annealing time curves at 310 and 300°C, respectively. Hereinafter, C vs. annealing time curves will be called C curves. One can see that *C(resistivity)* curve is almost equal to *C(yield stress)* curve at any post-annealing time. So the in-situ resistivity facilitates a real-time monitoring of yield stress for a sample during the annealing process. Both the C curves obtained from 310 and 300°C exhibit an exponential decay during the isothermal annealing, and reveal a flat at the end of the annealing. In addition, the slope of C curve increases with the annealing temperature, i.e., it takes less time to perform a full anneal on a sample at a high temperature. From the hall-patch equation[9-15], one can know that the yield stress is proportional to some power of grain size. For the deformed nickel, the increment of resistivity $\Delta\rho$ was determined by the following equation: $\Delta\rho = A + Bd^{-n}$, where A, B and n are constants[16]. Thus *C(resistivity)* and *C(yield stress)* are well fitted with each other, is relevant. Even when checked to industrial standards, the *C(resistivity)* curve measured from one sample is identical to the *C (yield stress)* curve tested from numerous samples via a tensile testing machine.

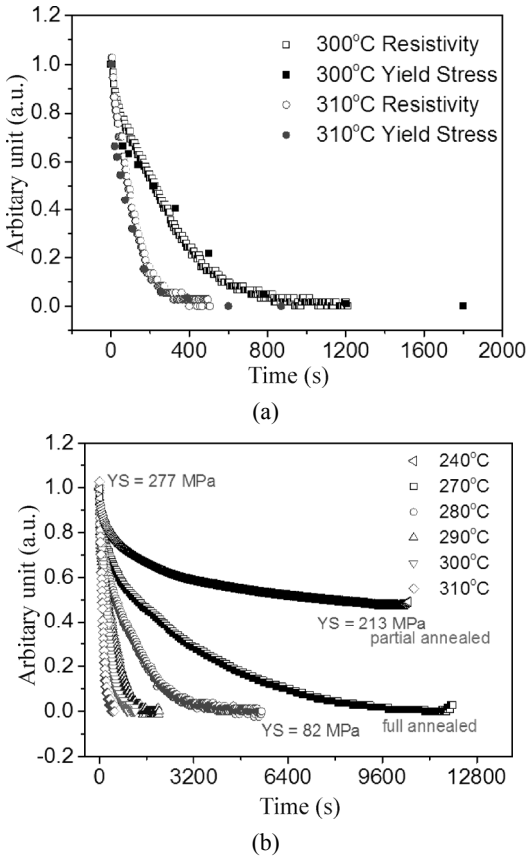

Fig.3. (a) *C(resistivity)* and *C(yield stress)* curves of 300°C and 310°C, respectively. (b) *C(resistivity)* curves from 250 to 310°C, respectively.

Figure 3(b) shows the *C(resistivity)* curves measured from 250 to 310°C. These curves manifest a detailed database which expresses the online resistivity as well as the yield stress during the annealing process. One can record the isothermal annealing history at various temperatures only with few samples. After proceeded with the in-situ resistivity measurement, aluminum sheets were fully annealed and revealed a yield stress value of 82 MPa. Noticeably, the sample annealed at 250°C is only partially annealed and exhibits a high yield stress value of 213 MPa. Therefore it can be said 250°C is the critical temperature for recrystallization, and then there is just the recovery phenomenon occurring in the lattice. It is the responsibility of the mill engineers to produce products which satisfy the mechanical specification required from their customers. With the C curves database, they can optimize the annealing time and temperatures under the considerations of energy consumption, heat transportation in the production annealing furnace, and required mechanical properties.

3.4 Optical images

Figure 4 shows optical images of the samples

annealed at 270°C for different times which are marked with square points as shown in the left inner figures. According to the tendency of the slope, the overall annealing history revealed in the inner figures are roughly divided into two regions. The sharp and flat slopes are subjected to the recovery and grain growth stages of the annealing process, respectively. Accordingly, the transition region with a moderate slope around the middle of y axis in *C* curve is caused from the recrystallization stage. Figure 4(a)-4(b) reveal the similar cold-rolled lamellar structure and there is no crystallization seed found in the grain boundaries, indicative of the pure recovery existing for 360-s and 1000-s annealing time. In Fig.4(c), the crystallization seeds appear more around the edge sites of the aluminum sheet, and the retained cold-rolled lamellar structures are observed in the middle site. It implies that the recrystallization phenomenon occurs for the sample corresponding to the 3000-s annealing treatment. When the annealing time is extended up to 10000 s, Fig.4(d) is full of the equiaxed grains when the grain growth stage is completed. Compared with optical images, the trend of the slope in *C(resistivity)* curve undoubtedly proves more useful information about the three stages of the annealing process in quantitative analysis.

3.5 Trend of decayed resistivity

In practical applications, a defect of the isothermal in-situ resistivity measuring needs to be solved. According to the Eq. (1), the time-dependent yield stress can be predicted from the *C(resistivity)* curve via interpolation method. It implies that the isothermal annealing process will last until the emergence of the final flat in the *C(resistivity)* curve. In order to skip the waiting time for the fully annealed status, one had better estimate the resistivity of fully annealed samples in the early period of annealing. Based on Eq. (1), a decayed resistivity is defined as $\frac{R_{instant} - R_{final}}{R_{initial}}$.

In Fig.5(a), the decayed resistivity vs. *T* appears as a linear relation from 255 to 310°C. However, a circle point acquired from the sample annealed at 250°C is obviously by far and away the main trend, manifesting the final states of the samples annealed at 250°C and 255-310°C result from different mechanisms, respectively. In accordance with the yield stress values tested from the annealed samples labelled in Fig.3(b), the aforementioned linear relation is proposed to be the fully-annealed trend, while the circle point shown in Fig.5(a) is suggested to be in the partially-annealed

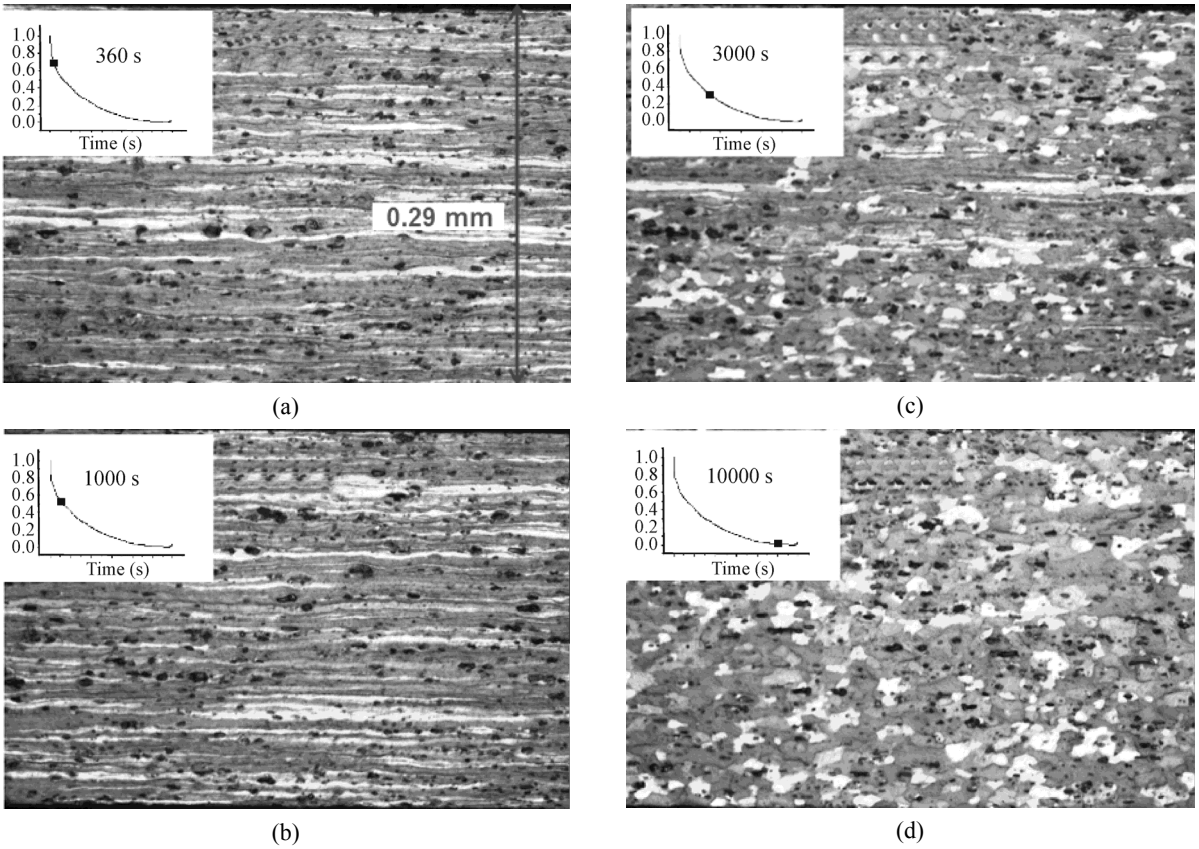

Fig.4. Optical images of etched samples annealed at 270°C for (a) 360 s, (b) 1000 s, (c) 3000 s, and (d) 10000 s, respectively.

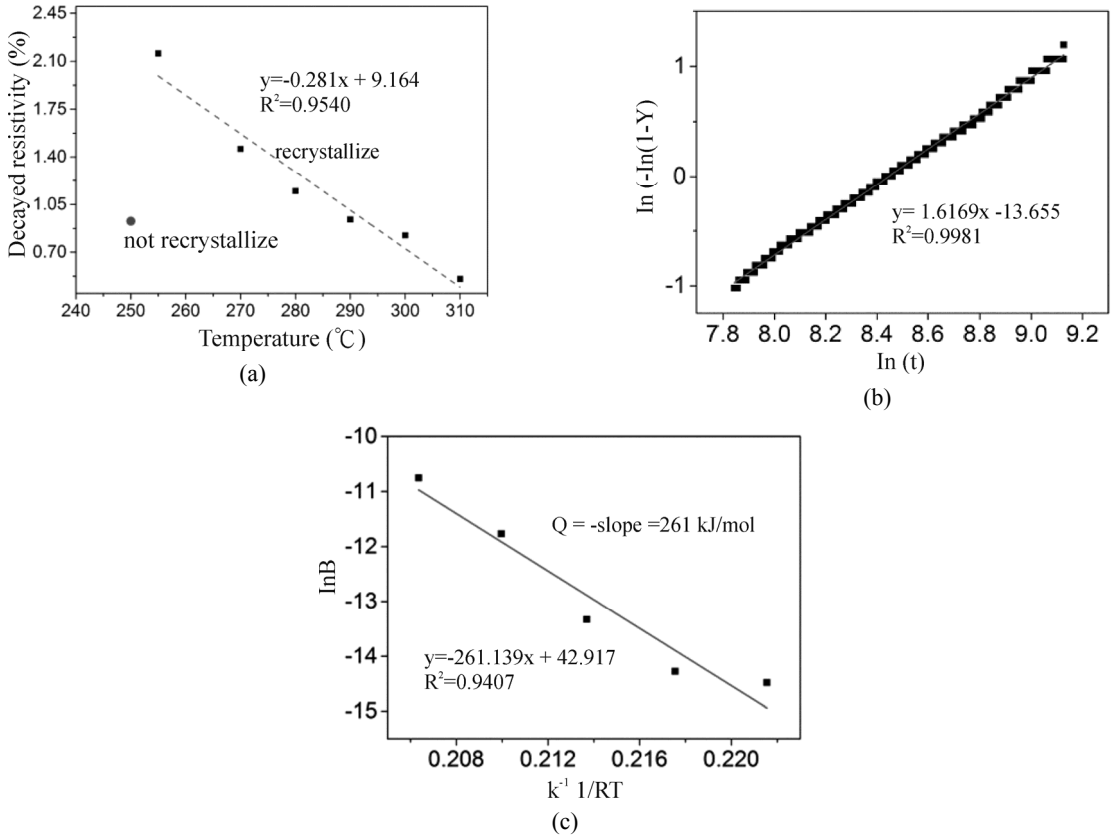

Fig.5. (a) The decayed resistivity vs. T plot, (b) The ln(-ln(1-Y)) vs. ln t plot of 270-°C annealed sample, (c) The ln B vs. 1 / RT plot.

region. With this fully-annealed trend, the investigator is able to interpolate the yield stress and the required annealing time in the early period of the *C(resistivity)* curve measuring when the operating temperature is higher than the critical recrystallization temperature. Also, the resistivity value obtained from the flat area of the *C(resistivity)* curve enables in checking if the sample is fully annealed.

3.6 Kinetics analysis

Since the aforementioned *C(resistivity)* curve is well fitted with the yield stress value at whichever time during isothermal annealing, it is granted to interpret *C(resistivity)* curve with Avrami equation which is usually applied to describe the kinetics of recrystallization softening behavior. A series of Avrami equations are defined as follows:

$$Y = 1 - \exp(-Bt^n) \quad \text{..... (2)}$$

$$\ln(-\ln(1-Y)) = n \ln t + \ln B \quad \text{..... (3)}$$

$$B = B_0 \exp(-Q / RT) \quad \text{..... (4)}$$

where Y is the volume fraction of recrystallization, B is the reaction rate constant, t is the annealing time, n is the Avrami exponent, B_0 is the pre-exponential factor, Q is the activation energy, R is the gas constant, and T is the given annealing temperature. Notice that Avrami equation is quite suitable for elucidating the period of annealing from recrystallization to grain growth. For aluminum alloys, the recrystallization usually initializes at around the time corresponding to $C = 0.5$[17,18], where C was mentioned in Eq. (1). Note that C in Eq. (1) is different from Y in Eq. (2). As illustrated in Fig.5(b), we used the raw data of in-situ resistivity to make the ln(-ln(1-Y)) vs. ln$t$ plot for the 270°C-annealed sample, and intentionally ignored the data on the end stage of grain growth. A linear fit with R^2 = 0.9981 was presented, and similar linear fit with $R^2 > 0.98$ happened to the samples annealed from 310 to 270°C. Based on Eqs. 3 and 4, the ln B vs. 1/RT plot was revealed as a linear line with R^2 = 0.9407 as shown in Fig.5(c). Consequently, activation energy Q can be figured out from the slope and the value is equal to 261 kJ/mol. On the similar basis of Avrami equation, the Q value of 3104 plate annealed at 500°C is only 155 kJ/mol[19]. Given these two 3104 aluminum alloys fabricated from simi-

lar chemical composition, Q decreasing with T is fairly reasonable. The Q value derived from via *C(resistivity)* curves will be a useful reference for investigators to predict the kinetics behavior of the sample before doing the next experiment.

4. CONCLUSIONS

Superior to DSC measurement which is only available in the environment of ascending temperature, in-situ electrical resistivity reflects the softening history of 3104 aluminum sheet during isothermal annealing. *C(resistivity)* and *C(yield stress)* curves well fitted with each other achieves the optimization in selecting the annealing temperature and annealing time for the production line. The *C(resistivity)*curves are revealed as an exponential decay and interpreted by the Avrami equation with $R^2 > 0.98$. From the slope of the ln B vs. $1/RT$ plot, the activation energy of the recrystallization is found to be 261 kJ/mol which is readily a reference for the future annealing experiment.

REFERENCES

1. K. Kazemi-Choobi, J. Khalil-Allafi and V. Abbasi-Chianeh, Investigation of the recovery and recrystallization processes of Ni50.9Ti49.1 shape memory wires using in situ electrical resistance measurement, Materials Science and Engineering: A, 551, 2012, pp. 122-127.
2. K. Mukunthan and E. B. Hawbolt, Modeling recovery and recrystallization kinetics in cold-rolled Ti-Nb stabilized interstitial-free steel, Metallurgical and Materials Transactions A, 27, 1996, pp. 3410-3423.
3. W. A. Johnson, Reaction kinetics in process of nucleation and growth, Transaction of AIME, 135, 1939, pp. 416-458.
4. A. N. Kolmogorov, On the statistical theory of the crystallization of metals, Bull. Acad. Sci. USSR, Math. Ser, 1, 1937, pp. 355-359.
5. T. McGill-Taylor, C. R. Brooks and S. Goodrich, Effect of cold working and annealing on mechanical properties and microstructure of hot rolled Al alloy 3104, Journal of Heat Treating, 9, 1991, pp. 5-25.
6. S. K. Vajpai and D. V. Malakhov, Investigation of Recrystallization via In-situ Electrical Resistivity Measurements, McMaster University, 2006.
7. N. M. McCurry, Aluminum temperature coefficient of resistance vs. grain structure, M.S. thesis of Lehigh Univ., 1993.
8. J. R. Davis, J.R.D. Associates and A.S.M.I.H. Committee, Aluminum and Aluminum Alloys, ASM International, 1993.
9. R. L. Fleischer, Substitutional solution hardening, Acta Metallurgica, 11, 1963, pp. 203-209.
10. W. Bragg, A theory of the strength of metals, Nature, 149, 1942, pp. 511-513.
11. H. Conrad, Effect of grain size on the lower yield and flow stress of iron and steel, Acta Metallurgica, 11, 1963, pp. 75-77.
12. J. P. Baïlon, A. Loyer and J. M. Dorlot, The relationships between stress, strain, grain size and dislocation density in Armco iron at room temperature, Materials Science and Engineering, 8, 1971, pp. 288-298.
13. A. Rohatgi, K. S. Vecchio and G. T. Gray, The influence of stacking fault energy on the mechanical behavior of Cu and Cu-Al alloys: deformation twinning, work hardening, and dynamic recovery, Metallurgical and Materials Transactions A, 32, 2001, pp. 135-145.
14. X. Feaugas and H. Haddou, Grain-size effects on tensile behavior of nickel and AISI 316L stainless steel, Metallurgical and Materials Transactions A, 34, 2003, pp. 2329-2340.
15. J. Aldazabal and J.G. Sevillano, Hall-Petch behaviour induced by plastic strain gradients, Materials Science and Engineering: A, 365, 2004, pp. 186-190.
16. T. Narutani and J. Takamura, Grain-size strengthening in terms of dislocation density measured by resistivity, Acta Metallurgica et Materialia, 39, 1991, pp. 2037-2049.
17. W. J. Poole, M. Militzer and M.A. Wells, Modelling recovery and recrystallisation during annealing of AA 5754 aluminium alloy, Materials Science and Technology, 19, 2003, pp. 1361-1368.
18. C. Sellars, A. Irisarri and E. Puchi, Recrystallization Characteristics of Aluminum-1% Magnesium Under Hot Working Conditions, in: Metallurgical Society of AIME Meeting, 1985, pp. 179-196.
19. F. Jiang, H. Zhang, C. Meng and L.-x. Li, Recrystallization of 3104 Aluminum Alloy during Compression at Elevated Temperature [J], Transactions of Materials and Heat Treatment, 32, 2011, pp. 52-55. □